

Oscillatory Interlayer Coupling and Magnetoresistance in Magnetic Metallic Multilayers

M. N. Baibich

Instituto de Física, Universidade Federal do Rio Grande do Sul, 91500, Porto Alegre, RS, Brasil

and

R. B. Muniz

Instituto de Física, Universidade Federal Fluminense, 24020, Niterói, RJ, Brasil

Received October 20, 1992

The oscillations of the interlayer exchange coupling and the giant magnetoresistance effect in magnetic metallic multilayers have been intensively investigated both experimentally and theoretically. The current status of the theory and some specific experimental results concerning these systems are briefly reviewed.

I. Introduction

Different metals can be deposited in consecutive layers to form what are generally called metallic multilayers. These systems may exhibit physical properties which are very different from those of their constituent materials. With the development of new experimental techniques and refined control in materials science, it is now possible to monitor the growth and characterize these structures within an atomic scale¹. Careful control of growth can produce systems with new periodicities, effectively of low dimensionality, and may place elements in stable structural phases in which they are not usually found in nature. Such new boundary conditions may greatly alter the underlying electronic structure, and hence the properties of these materials². The design of new materials requires a constant interplay between theory and experiment.

The magnetic properties of metallic multilayers composed by magnetic and non-magnetic metals may be used to produce devices of great interest for the magnetic industry. For example, the magnetic anisotropy at the interface between metals like Co/Pt and Ni/Pt³ can favor perpendicular magnetization, which is useful for producing high-density storage medium. An applied magnetic field can cause big changes in the resistance of certain magnetic metallic multilayers, and this effect may be exploited to construct magnetic sensors. Early magnetoresistive sensors were based on materials which show approximately 2% change in resistance, but in some metallic multilayers the change can be as high as 100%. This unexpectedly high effect has been called giant magnetoresistance and was first observed in Fe/Cr multilayers by Baibich et al⁴.

It has also been observed^{5,6} that the coupling between the magnetic layers of metallic multilayers may be either ferromagnetic or antiferromagnetic depend-

ing on the thicknesses of the spacer layers. The period, phase and magnitude of the oscillations of the interlayer coupling, as well as the magnetoresistance, depend on the multilayer constituent materials, and interface quality may also play a very important role.

Here, we shall concentrate on magnetic metallic multilayers composed by ferromagnetic transition metals separated by non-magnetic transition or noble metal. Our attention is devoted to two magnetic properties observed in these multilayers, namely the oscillations in the interlayer coupling and the giant magnetoresistance effect.

II. Samples and Experimental Methods

Careful control of multilayer growth requires a great deal of science and not less of art. Most of the evaporation methods traditionally used to prepare thin films may also be employed to produce multilayers. The essential problem in growing these structures is to have a good control of the thicknesses, interface roughness and chemical purity of the layers.

Initially, fairly sophisticated methods like the Molecular Beam Epitaxy (MBE) were used to prepare good quality samples. Later, it was found that some of the properties originally attributed to the single crystal structures obtained by MBE were also present in polycrystalline samples. More recently, it has been shown that even the epitaxy of certain metallic multilayers can be obtained with standard electron beam physical deposition machines⁷. These much simpler, faster and economical methods of sample preparation increase the potential technological application of these systems in the magnetic industry.

Multilayers with translational symmetry in the direction perpendicular to the layers are called superlattices. Polycrystalline multilayered samples retain the

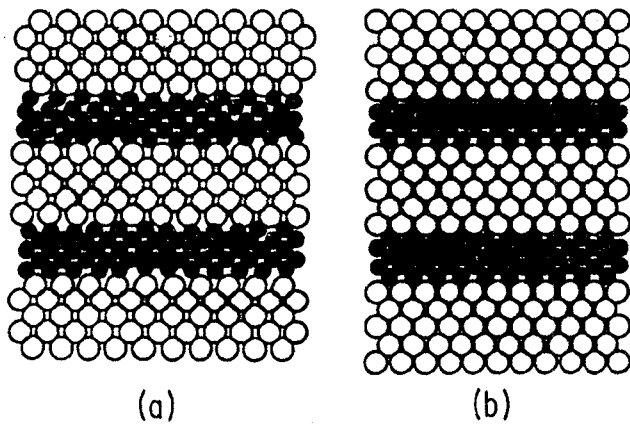


Figure 1.: Schematic representation of two-component superlattices (a) polycrystalline sample (b) single crystal structure (after Draaisma ref. [8]).

compositional symmetry but not a unique crystal orientation, although they are usually predominantly textured in one direction. This is schematically shown in Fig. 1. One of the most useful and powerful methods for investigating the underlying symmetries of these systems is X-ray diffraction (XRD). Both small and large angles XRD provide information about the periodicity of the system and quality of its interfaces. Ideally, XRD patterns of a two component superlattice show either two intensity distributions (each centered around the corresponding Bragg peaks of the constituent materials), or a distinct intensity distribution around an average Bragg peak in the cases of large and thin layer thicknesses, respectively. These Bragg peaks are decorated by equally spaced satellite peaks associated with the chemical period of the bilayer. Deviations from the ideal situation can be analyzed with more refined models to obtain information about the sample texture, and roughness of the interfaces. Other experimental techniques, such as nuclear magnetic resonance (NMR) and Mössbauer spectroscopy look at changes in the hyperfine fields at suitable isotopes, and in some cases may be used to acquire additional information about the local structure and magnetic properties of the system.

III. Magnetic properties

The magnetic properties of layered structures can be studied by different experimental methods such as neutron scattering, Brillouin scattering, spin polarized low energy electron diffraction (SPLEED), ferromagnetic resonance (FMR), and by magneto-transport, magnetization and torque measurements. Ferromagnetic and antiferromagnetic alignments of the magnetic layers lead to different behaviors of the magnetization M as a function of an applied magnetic field H . The hysteresis loop shown in Fig. 2, where the remanent magnetization is hardly visible and the saturation field is

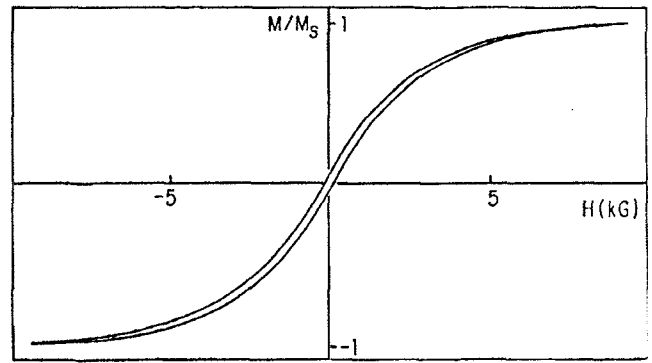


Figure 2.: Magnetization vs. in-plane field for Fe(30 Å)/Cr(12 Å) superlattice at 4.2 K (from ref. [4]).

relatively high, is characteristic of an antiferromagnet. In a ferromagnetic configuration the system saturates at low fields and the slope of M at $M \cong 0$ is much steeper. Magnetization measurements of this kind have been used to establish whether the interlayer coupling in magnetic metallic multilayers is antiferromagnetic or not. This may be confirmed by other experimental technics such as light scattering⁹, SPLEED¹⁰, neutron diffraction¹¹, and observations of the magneto-optical¹² and planar Hall effects⁴. Also, the magnitude of the interlayer exchange coupling in the antiferromagnetic configuration can be obtained from the observed value of the saturation field as follows¹³. The energy of two magnetic layers with magnetizations $\vec{\mu}_1$ and $\vec{\mu}_2$ coupled by exchange interaction J in the presence of a magnetic field H is

$$E = -J\vec{\mu}_1 \cdot \vec{\mu}_2 - H \cdot (\vec{\mu}_1 + \vec{\mu}_2), \quad (1)$$

where $\vec{\mu}_1$ and $\vec{\mu}_2$ are the unit magnetization vectors. Let us consider the case where both $\vec{\mu}_1$ and $\vec{\mu}_2$ are parallel to the layers. With the in-plane field H perpendicular to the magnetization axis, the saturation field H_s is obtained by imposing that the minimum of E occurs when both $\vec{\mu}_1$ and $\vec{\mu}_2$ are parallel to H . It follows that the exchange coupling per unit area A between the magnetic layers is given by

$$J \equiv J/A = -H_s M_s t_M / 2, \quad (2)$$

where M_s and t_M are the magnetization per atom and the thickness of the magnetic layer, respectively.

The measured values of J obtained in this way are, for example, $J = -2.8$ ergs/cm² in Fe/Cr(9 Å), $J = -0.24$ ergs/cm² in Co/Cu(95 Å), and $J \cong -5$ ergs/cm² in Co/Ru(35 Å). These relatively high values of J cannot be accounted for simply by magnetostatic interaction. Just for comparison, the estimated value of J between nearest neighbor bulk iron atomic planes is $\cong 18.9$ ergs/cm².

It has been found that the sign and magnitude of the interlayer coupling depend on the spacer layer thick-

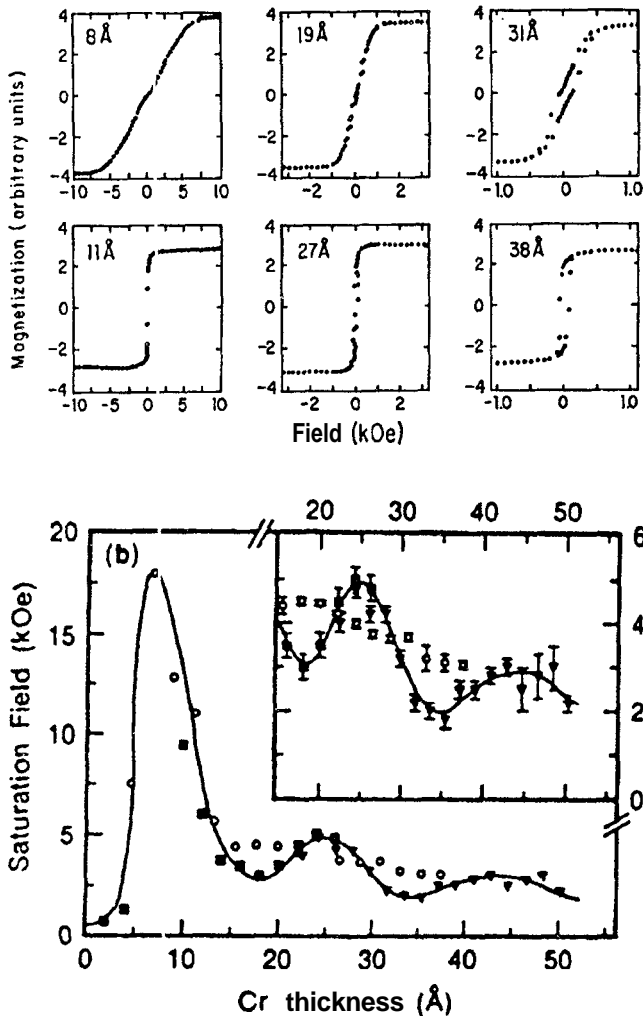


Figure 3.: (a) Magnetization (300K) vs. in-plane field for $\text{Co}(18 \text{ \AA})/\text{Ru}(t_{\text{Ru}})$ superlattices for some values of t_{Cr} as indicated in the figures; (b) Saturation field (4.2 K) vs. Cr layer thickness for $\text{Fe}(20 \text{ \AA})/\text{Cr}$ superlattices. Taken from ref. [6].

ness. In fact, Parkin et al.⁶ discovered that the inter-layer coupling oscillates with an overall decreasing amplitude, as the spacer layer thickness increases (Fig. 3). The period of oscillations in sputtering grown samples can be rather large, e.g. $\cong 20 \text{ \AA}$ in Fe/Cr ⁶, and $\cong 12.5 \text{ \AA}$ in Co/Cu or Fe/Cu . This behavior has been confirmed by light scattering measurements¹⁴.

More recently, the Jülich group devised a very ingenious sample in which a Cr wedge is deposited over an iron single crystal whisker and subsequently covered by an Fe overlayer. In this way, the Cr thickness is almost continuously varied, and Fe interlayer couplings through different Cr thicknesses are realized in a single sample. Both Purcell et al.¹⁵ and Demokritov et al.¹⁶ have observed, by magneto-optical Kerr effect (MOKE) measurements in this kind of a sample, a period of about two monolayers apparently superimposed on a long period comparable to that previously seen

by Parkin et al.⁶. In a beautiful experiment Unguris et al.¹⁷ used scanning electron microscopy with polarization analysis (SEMPA) to demonstrate that the interface quality plays a decisive role as far as the period of oscillation in this system is concerned. They obtain both short and long period oscillations in the coupling by varying the quality of the wedge structure, as shown in Fig. 4. Poorer quality interfaces apparently introduce irregular local variations in spacer thickness which wash out short period oscillations. With flat interfaces other superlattices present short period oscillations superimposed to long ones¹⁸.

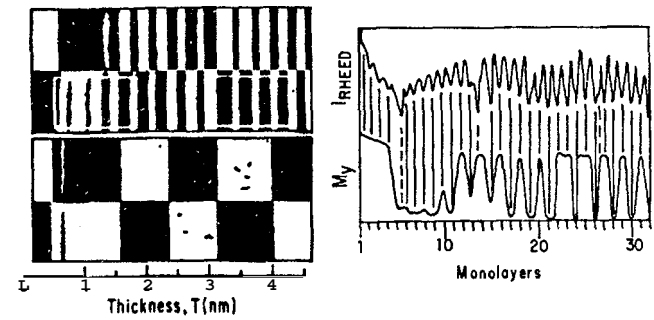


Figure 4.: (a) SEMPA images of the magnetic coupling of the Fe layers in two $\text{Fe}/\text{Cr}/\text{Fe}$ wedge samples with different crystalline qualities. The image in the upper panel refers to the well ordered Cr layer spacer and shows short period oscillations in the coupling. The lower panel image refers to the poor quality sample and shows the same period as that obtained with sputtering grown samples^{6,14}. (b) Magnetization and RIEED oscillations corresponding to the good quality sample of part (a). The oscillations in M_y line up with the RIEED. Taken from Unguris et al. (ref. [17]).

The period, phase, and amplitude of the oscillations depend on the multilayer constituent materials and also on the crystal direction of growth^{18,19}. Phase and period changes occur between the (111) and (100) directions in Co/Cu , and (100) Fe/Cu superlattices²⁰, as shown in Fig. 5.

IV. Electronic Transport Properties

Measurements of electronic transport properties in metallic multilayers often require the same precautions as in metallic thin films. The electrical currents must be small to avoid layer damages and the experimental geometries used must take into account the fact that total thickness of these multilayer samples are usually small.

A classical theory for the conduction in thin films and wires in the absence of a magnetic field was developed by Fuchs and Sondheimer²¹, and later adapted to superlattices by Carcia and Suna²². The presence of an applied magnetic field alter the electron motion causing the conventional magnetoresistance effect. On the

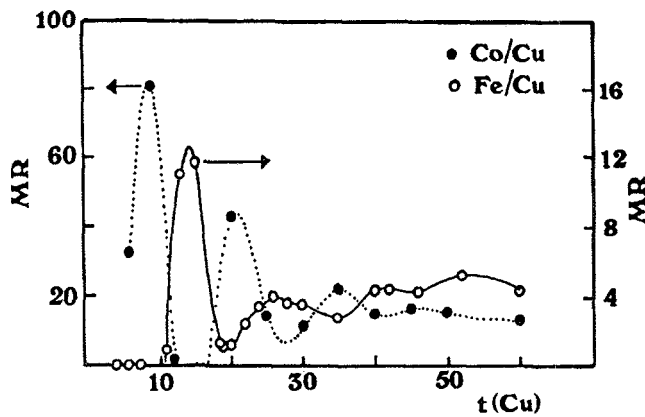


Figure 5.: Variation of the magnetoresistance ratio of both Fe(15 Å)/Cu(t_{Cu}) (open symbols) and Co(15 Å)/Cu(t_{Cu}) (full symbols) superlattices as a function of the Cu layer thickness. Dotted and full lines are just eye guides. Taken from Petroff et al. (ref. [20]).

Other hand, the resistivity of magnetic materials may depend on the direction of the current relative to the magnetization axis. This effect is also called magnetoresistance but, in this case, the main role of the field is not to influence the electron motion but merely to align the magnetic moments. The difference in resistivities for currents flowing parallel and perpendicular to the magnetization in traditional materials are relatively small, not exceeding 3%. However, in some magnetic metallic multilayers a dramatic change in resistance can be produced by applying a magnetic field which alters the magnetic configuration of the system. A giant effect of this type was observed in Fe/Cr superlattices by Baibich et al.⁴. They have studied samples grown by MBE in the (100) direction, where the magnetization of the Fe layers lie in the plane of the layers. They have measured the change in resistance as a function of applied magnetic field with the current also in the plane of the layers. No significant difference was found between the cases where the current is parallel or perpendicular to the field. For 9 Å Cr thickness corresponding to an antiferromagnetic coupling between the Fe layers they have observed, at low temperatures, a change of almost a factor of two between the resistivities at zero field and in the saturated state. The same change in resistance was obtained with the applied field perpendicular to the layers, although a higher field is necessary to saturate the system, because in this case it needs to overcome both the antiferromagnetic coupling and the anisotropy which makes the magnetization to be in the plane of the layers. Typical results are shown in Fig. 6.

Giant magnetoresistance effect have been observed also in several other magnetic metallic multilayer systems^{6,23}. Most of the magnetoresistance measurements in these systems are performed with the current flowing in the plane of the layers, but recently

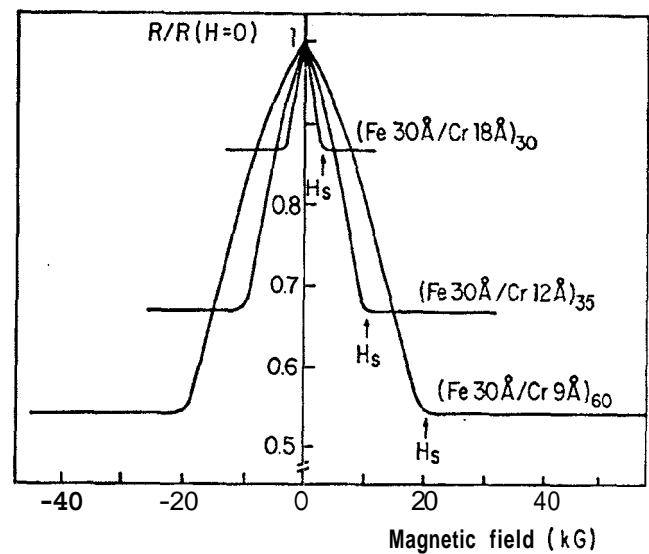


Figure 6.: Magnetoresistance of Fe/Cr superlattices at 4.2 K. Current and magnetic field are in the plane of the layers. Taken from Baibich et al. (ref. [4]).

Pratt et al.²⁴ have shown that the magnetoresistance of Co/Ag measured with the current perpendicular to the layer planes can be more than ten times as large as the current-in-plane magnetoresistance of the same sample. Their measurements require special techniques such as SQUID detection because of the very small voltages and resistances involved.

The saturation magnetoresistance ratio is defined as

$$\Delta R/R = [R(H_c) - R(H_s)]/R(H_s), \quad (3)$$

where H_c is the coercive field and H_s is the saturation field. It is interesting to note that the original definition used by the Orsay group was $[R(0) - R(H_s)]/R(0)$. Thus, their published data for the magnetoresistance of Fe(20 Å)/Cr(12 Å) multilayer is a factor of two bigger than that observed by Parkin et al.⁶ for the same system. The difference seems to be due to fact that they have used different samples, grown by MBE and sputtering methods respectively. However, one would generally expect MBE samples to have sharper interfaces than those prepared by sputtering, and hence less interface roughness. The role played by interfacial roughness in the magnetoresistance is not yet fully understood. Direct experimental attempts to determine whether introducing interface roughness increases or decreases $\Delta R/R$ are still inconclusive. In some cases, it seems that a certain amount of roughness is necessary to maximize the magnetoresistance effect, as schematically shown in Fig 7²⁷. But, as pointed out by Parkin (private communication), one must be careful in analyzing these experiments because small changes in the spacer thickness around a magnetoresistance maximum can place the sample below or above the magnetoresistance peak.

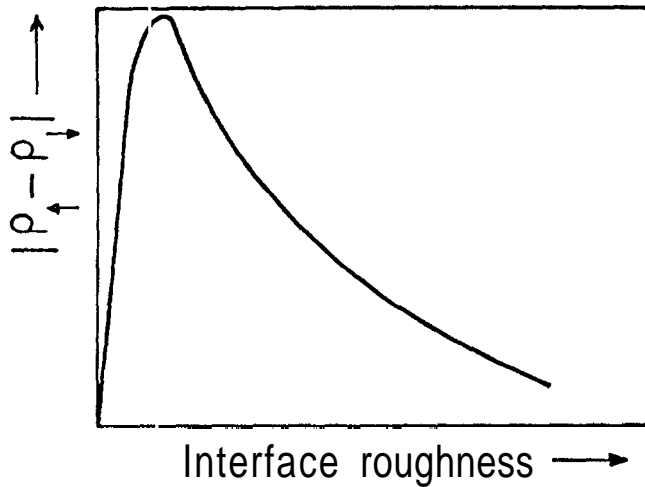


Figure 7.: Qualitative sketch of the spin dependent interface scattering difference as a function of interface roughness. Taken from ref. [26].

Growth conditions may influence the quality of the samples introducing some dispersion in the experimental data. Nevertheless, it is undisputable that the magnetoresistance effect can be very large in some magnetic metallic multilayers. In Fig. 8 we show the results of $\Delta R/R$ in Co/Cu superlattices as a function of the Cu thickness, measured with the current in the planes of the layers. The observed oscillations in $\Delta R/R$ are associated with the oscillations in the interlayer coupling. For large Cu thicknesses, the oscillations seem to disappear, and just an overall decrease in $\Delta R/R$ persists. Zhang and Levy²⁷ explains this behavior by arguing that when the coupling is not sufficient strong to define a single magnetic configuration of the multilayer structure, it is necessary to consider an average over all possible configurations.

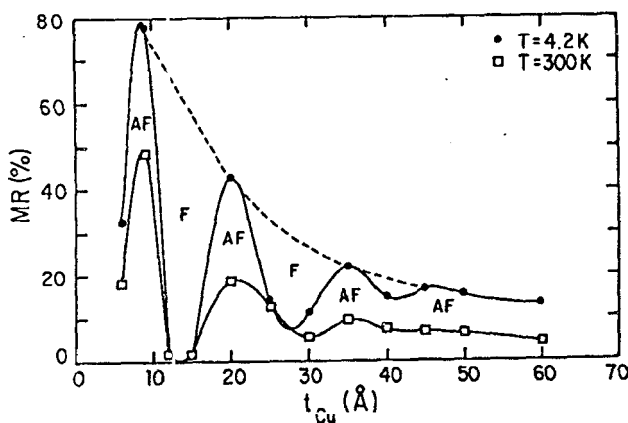


Figure 8.: Variation of the magnetoresistance ratio of Co(15 Å)/Cu(t_{Cu}) superlattices as a function of the Cu layer thickness. Taken from D. H. Mosca et al. (ref. [23]).

V. Oscillation in the exchange coupling

As we have previously mentioned, the magnetic moments of adjacent ferromagnetic layers composed by metals such as Fe and Co separated by a non-magnetic metallic layer can couple ferromagnetically or antiferromagnetically depending on the thickness of the spacer layer. Early work^{5,28} indicated a monotonic decrease in the antiferromagnetic coupling between the magnetic layers with increasing thickness of the spacer layer. However, Parkin et al⁶ discovered that the coupling in Co/Ru, Co/Cr, and Fe/Cr superlattices actually oscillates between ferromagnetic and antiferromagnetic as the spacer layer thickness increases. This oscillatory behavior was subsequently observed by different groups in a wide variety of other metallic systems^{14,23,29}. We have also mentioned that the strength of the antiferromagnetic coupling is, in most cases, sufficiently high to exclude a possible magnetostatic origin. Also, the rather large exchange coupling period ($\approx 10 - 20 \text{ \AA}$) initially observed in some multilayers caused surprise, because a naive application of a continuous and free electron gas Ruderman-Kittel-Kasuya-Yosida (RKKY) theory gives much shorter periods. These facts motivated several theoretical and experimental works aimed at understanding the origin of both the exchange coupling and its long period of oscillations in those metallic multilayers.

Generally, the exchange coupling can be determined by the difference in total energy between the ferromagnetic and the antiferromagnetic configuration of the system. Direct numerical calculations of the total energies, however, must be performed with very high accuracy because the energy differences are extremely small in comparison with the total energies involved. Hence, the degree of complexity in treating the underlying electronic structure and the method of calculation used may severely restrict the range of systems which can be practically treated by this approach. For instance, Hasegawa³⁰ found that the required accuracy to compute the exchange coupling is very hard to achieve even with a simplified tight-binding d-band model. First principles calculations based on local spin density functional theory have been carried out^{31,32} for some superlattices but the calculated exchange coupling is one or two orders of magnitude larger than observed. Stoeffler and Gautier³³ used a multi-orbital tight-binding model to calculate the total energies of various multilayers but their results are also large when compared with the experimental values. Presently these calculations are restricted to thin layer thicknesses and hence still unsuitable to investigate long period oscillations. Model calculations with simpler band structure are important because they may reveal the relevant physical mechanisms often hidden behind extensive first-principles numerical computations. Along this line Edwards et al.³⁴⁻³⁶ considered a simple model and developed a theory for the coupling across a transition metal spacer which exhibits

many of the observed features of the oscillatory inter-layer coupling.

Here, for presentation purposes, we distinguish between noble and transition metal spacers and divide existing theoretical works into two different (but in our view complementary rather than competing) types of approach. Theories of the exchange coupling based on total energy calculations like the ones we have briefly mentioned, and RKKY-type of theories in which the exchange interaction between localized moments mediated by conduction electrons are calculated by perturbation theory³⁷⁻⁴².

For noble metal spacers, with the d bands well below the Fermi level and a broad nearly-free-electron sp conduction band, it is difficult to conceive anything much different from a RKKY-like coupling. As a second order perturbation theory, RKKY is not expected to provide a good description of the coupling for thin spacer layer thicknesses. However, in this case, first-principles total energy calculations has a chance of yielding accurate results for the coupling. On the other hand, in the opposite limit (i.e. for very large spacer layer thicknesses) total energy calculations are very hard to deal with numerically, but RKKY may provide a much simpler approach. Nevertheless, it is difficult to calculate the strength of the coupling within RKKY, where usually the value of the coupling ultimately depends on a rather arbitrary choice of values for the parameters involved.

Asymptotic behavior concerning the period of oscillation, rate of decay and temperature dependence obtained from RKKY⁴⁰ agree with the model calculations of Edwards et al^{34,35}. In both theories the occurrence of long period oscillations in the exchange coupling is intimately associated to the discrete nature of the spacer layer. For a one-band tight-binding model with nearest plane hopping, and layer orientation corresponding to a plane of reflection symmetry in the spacer, Edwards et al³⁵ showed that the period of oscillation is determined by caliper measurements of the spacer Fermi surface normal to the layer planes, and long-periods arise when the Fermi surface is close to the zone boundary. Coehoorn⁴³ (see also Chiappert and Renard⁴⁴) drew similar conclusions by analyzing in real space the ratio between the period of the spin density oscillations induced in the conduction electrons and the discrete spacer layer thickness.

The RKKY range function in a planar geometry may be calculated⁴⁵ by taking the one dimensional Fourier transform of the wavevector-dependent susceptibility $\chi(q = 0, q_z)$, where q and q_z are the components of the wave vector parallel and perpendicular to the layers respectively. Asymptotically, significant contributions to the range function mainly comes from wave vectors which maximize χ , hence long period oscillations in the interlayer coupling are associated with singularities in $\chi(q_z)$. Bruno and Chappert⁴⁰ have analyzed bulk

Fermi surfaces of Cu, Ag and Au in an extended zone scheme to identify the extrema in χ and determined the relevant wave vectors for the interlayer coupling periods of oscillations in different crystalline orientations. For (111) Cu spacer layer they predicted a unique period of $\approx 9.4 \text{ \AA}$ in very good agreement with the value observed in Co/Cu samples predominantly textured in the (111) direction²³.

For transition metal spacers with partially filled d-bands there is no reason to expect a simple nearly-free-electron like polarization of the type usually considered by RKKY. A complete treatment of the polarization involving the d-bands would be much more involved. Wang et al³⁹ used a theory⁴⁶ originally developed for rare earth compounds to study the interlayer coupling in Fe/Cr. In their calculations they have used full band structure of bulk paramagnetic Cr but the \uparrow and \downarrow spins Fe d-bands were substituted by atomic levels located below and well above the Fermi energy respectively. The magnitude of the coupling was found to be strongly dependent on the estimated values of the position of the \uparrow spin Fe d-level relative to the Fermi energy, and a second parameter was used to set the final coupling energy scale. Ferromagnetic transition metals separated by transition metal spacers should have their d-bands treated on equal footing, and preferably within an itinerant picture because they are not localized. Consequently, in this case, a more careful treatment of the electron spin interactions is required.

We now briefly describe the theory of Edwards et al³⁶ for the interlayer coupling across a transition metal spacer. For this purpose, it is sufficient to consider two semi-infinite transition metal ferromagnets separated by a transition metal spacer containing N atomic planes. The exchange coupling $J(N)$ is given by the difference in energy, per unit area of the layers, between the ferromagnetic and antiferromagnetic configurations of the sandwich. For simplicity it is assumed that d-bands contributions to the energies are dominant and hence the sp conduction band is omitted; total energies of the two configurations are approximated by one-electron energy sums. The Fermi level is fixed by the bulk ferromagnets and the spacer aligned accordingly. Changes in the d-levels in each atomic plane with respect to their appropriate bulk values are neglected, thereby avoiding a self-consistency which would slightly change these levels near the interfaces. To make the calculations even simpler we further assume the same d-band width for both magnetic and non-magnetic metals, and that the number of \downarrow spins electrons per atom in the magnetic metal is equal to the number of electrons per atom of either spins in the non-magnetic metal. To emphasize the basic physical mechanism we initially consider the case in which the \uparrow spin electron d band of the ferromagnet is full. In such a case, when the sandwich is in the ferromagnetic configuration, the \uparrow spin holes experience a constant potential throughout

the structure, whereas \downarrow spin holes feel a potential well in the spacer layer. The well is caused by the exchange field which increases the number of \uparrow spin electrons in the ferromagnets in both sides of the sandwich in the parallel configuration, hence reducing the \downarrow spin holes occupation in these regions. The presence of the well confine the \downarrow spin holes essentially in the non-magnetic spacer metal, and introduces size quantization effects which clearly depend on the spacer layer thickness. When the sandwich is in the antiparallel configuration, \uparrow spin holes experience a potential step when crossing the second interface, and \downarrow spin holes feels a similar step when crossing the first interface. It follows that, in this configuration, \uparrow spins holes are confined in the half space to the left of the second interface, and \downarrow spin holes in the half to the right of the first interface. The situation is schematically shown in Fig. 9 for both configurations and spin directions. The well depth, and heights of the two steps, depend on the exchange splitting of the ferromagnets and control the effectiveness of the confinements. A very simple model is to consider the on-site interaction $U = \infty$ in the magnetic layers and $U = 0$ in the spacer layer. In this case, \downarrow spins holes are completely confined in the spacer layer in the ferromagnetic configuration, and the cost in energy to produce such a confinement clearly depends on the spacer thickness. On the other hand, in the antiferromagnetic configuration, the half space confinement of each spin holes is caused by a single surface term, and hence the associated cost in energy is independent of the spacer thickness. Therefore, qualitatively, it is then conceivable that the energy cost to obtain a ferromagnetic configuration may be sometimes higher sometimes lower than the antiferromagnetic one, depending on the spacer layer thickness.

The interlayer coupling is proportional to the energy difference between the parallel and antiparallel configurations of the sandwich, with constant hole number, and is given by

$$J(N) = [\Omega(N) - \Omega(\infty)]/A \quad (4)$$

where $\Omega(N)$ is the free energy which at zero temperature reduces to

$$\Omega(N) = E(N) - E_F n(N). \quad (5)$$

Here, $E(N)$ is the total energy of the \downarrow spin holes confined in a spacer with N atomic planes, measured relative to a reference state with N bulk planes; $n(N)$ is the corresponding number of holes; E_F is the Fermi energy, $\Omega(\infty)$ is the constant (N independent) surface term present in the antiferromagnetic configuration, and A is the area of the layers. At zero temperature $\Omega(N)$ may be calculated by

$$\Omega(N) = \int_{-\infty}^{E_F} (E - E_F) \Delta\rho(E) dE, \quad (6)$$

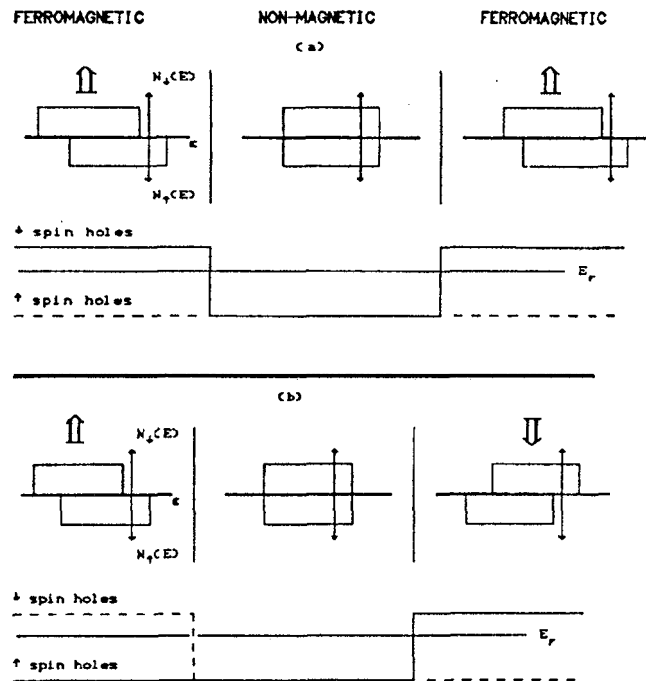


Figure 9.: Schematic representation of the densities of states for each spin $N^\uparrow(E)$ and $N^\downarrow(E)$ in each region of a sandwich for (a) ferromagnetic and (b) antiferromagnetic alignments of the magnetic layers; the vertical axis is drawn at the Fermi level E_F . Inset: Schematic plots of the potentials experienced by the holes of different spins in each case (dashed line for \downarrow spin holes, solid line for \uparrow spin holes).

where $\Delta\rho$ is the change in the density of states of the confined holes relative to bulk reference system.

The confinement quantizes the \downarrow spin hole states in the direction perpendicular to the layers and this shows up as steps in the corresponding density of states. The number, heights and position of these steps depend on the width of the well, as in the case of a film where they depend on the film thickness. As the spacer layer thickness changes, these steps move and may cross the Fermi level, leading to oscillations in the exchange coupling. The situation is similar to the de Haas-van Alphen (dHvA) effect in which oscillations are associated with the quantization produced by an applied magnetic field. Here, the quantization is imposed by the exchange field and the variation of the spacer thickness causes the quantized states to pass through E_F . Exploiting this analogy with the dHvA, and considering a simple one-band tight-binding model with nearest plane hopping, and layer orientation corresponding to a plane of reflection symmetry in the spacer, Edwards et al. derived the following asymptotic formula for the interlayer coupling

$$J(N-1) = \frac{1}{4\pi N a} \operatorname{Re} \sum_{s=2}^{\infty} \frac{\sigma}{s^2} \left| \frac{\partial k_z^2}{\partial k_x^2} \cdot \frac{\partial k_z^2}{\partial k_y^2} \right|^{-1/2} \times \frac{\exp[2i s N a k_z^0(\mu)]}{T^{-1} \sinh [2\pi s N a T \frac{\partial k_z}{\partial \epsilon}]} \times \begin{cases} \text{both 2nd derivatives} > 0 \\ i, & \text{both derivatives} < 0 \\ 1, & \text{one derivative} > 0, \text{ the other} < 0. \end{cases} \quad (7)$$

The formula is valid for finite temperature T as well as $T = 0$, and it is exact for this particular model, where $U = \infty$ in the magnetic metals and equal to zero in the spacer layer. Here, $k_z^0(\mu)$ is an extremal radius of the Fermi surface in the direction perpendicular to the layers (half the caliper measurement) and all the derivatives in Eq. 7 are taken at the stationary point k_z^0 & $k_x^0(\mu), k_y^0(\mu)$; a is the lattice parameter and μ the chemical potential fixed by the ferromagnets (at $T = 0$ $\mu = E_F$). The consequences of this asymptotic formula for $J(N)$ are:

- (i) The period of oscillations in the exchange coupling is determined by the factor $\exp[2i N a k_z^0(\mu)]$. Clearly, owing to the discrete thickness $N a$ of the spacer layer, $k_z^0(\mu)$ may be replaced by $k_z^0(\mu) - \pi/a$. Therefore, long periods are obtained either when the radius $k_z^0(\mu)$ is small or when the Fermi surface approaches the zone boundary at π/a so that $k_z^0(\mu) - \pi/a$ is small.
- (ii) The amplitude contains a factor of the Fermi surface at its extremal points.
- (iii) The temperature dependence of the oscillations is governed by the velocity of carriers at the extremal points.
- (iv) The asymptotic decay at $T = 0$ is proportional to $1/N^2$ but becomes exponential at finite T .

Numerical calculations for specific cases of a one-band model and simple cubic (100) orientation of the layers at $T = 0$ show that the asymptotic formula given by Eq. 7 is rather accurate for $N > 5$. In this case, long period oscillations are obtained for $E_F \cong -1$, which corresponds to a situation where the Fermi surface is close to the zone boundary. For $E_F = -1.05$ the sign of J for $N \cong 5$ is antiferromagnetic, and the period is $\cong 10$ interatomic distances, which is close to what was observed in structures like Co/Ru³. Also, the magnitude of J , calculated with this value of E_F and for a spacer thickness of a few atomic planes, is $\cong 1$ erg cm⁻², which is of the order of magnitude of the Co/Ru measured value.

For $E_F = -0.95$ the period is again long, but there is a phase shift in the oscillations compared with $E_F = -1.05$. For $E_F > -1$, the Fermi surface develops four necks in the plane parallel to the layers (equivalent to two saddle points) and the diameter of the necks is small for $E_F = -0.95$. These necks are the extrema that determine the oscillations in the exchange coupling for $-1 < E_F < 0$, and the phase shift is obtained because

the factor σ in Eq. 7 takes a value $\sigma = 1$ for a saddle point.

Short period oscillations can be obtained for example with $E_F = -2.5$. In this case the amplitude of oscillations is bigger than those with $E_F \cong -1$ because of the greater curvature of the Fermi surface at the extremum. In practice, roughness of the surfaces may lead to a variable effective spacer thickness which would tend to suppress short-period oscillations, such as those with $E_F = -2.5$, due to an averaging effect.

The theory described so far was developed assuming a complete confinement of holes. This is a very stringent assumption which clearly should be relaxed for a weak ferromagnet like Fe which has d -holes in both minority and majority spin bands. In this case, holes are not totally confined inside the spacer layer, neither in half spaces. To investigate the effect of partial hole confinement³⁶, we need to consider a finite exchange splitting V in the magnetic layers. For simplicity, we avoid a full self-consistent treatment of the problem and assume a simple picture in which the effective on-site energies are taken to be zero inside the spacer layer, and either V or 0 inside the magnetic metals, depending on the configuration and spin directions of the holes. Thus, the steps at the interfaces have height V , and basically two situations may occur. The first, which is pictured in Fig. 9, is when $E_F < V$ as in Co. In this case, for finite V , \downarrow spin holes can penetrate a few layers across the interfaces inside the magnetic metals in the ferromagnetic configuration; the confinement will not be precisely restricted to the spacer layer, but still will be essentially within a finite region. Similar penetrations will also happen in the antiferromagnetic arrangement through the corresponding finite potential step experienced by holes of either spins. The other situation is when $E_F > V$. In this case, there are holes of both spins in the magnetic metals (as in Fe), and they are only partially reflected by the potential steps at the interfaces. In the ferromagnetic configuration resonances may occur in the \downarrow spin holes for a fixed value of V as the spacer thickness vary.

To calculate the interlayer coupling at $T = 0$, we can still use Eqs. 4-6, but a Green function method is required to calculate A_p ³⁶, which is then given by

$$\Delta\rho = (-1/\pi) \sum_k \operatorname{Im} \sum_n \Delta G_{nn}(E, k), \quad (8)$$

where $\Delta G_{nn}(E, k)$ is the difference between the diagonal element of the Green function in atomic plane n and the appropriate reference bulk Green function, and k is a two-dimensional wave vector parallel to the layers. For the ferromagnetic configuration where the \downarrow spin holes move in a potential well of depth V we may rewrite

$$\sum_n \Delta G_{nn}(E, k) = \operatorname{Tr}[\partial \ln(1 - G^0 V)/\partial E], \quad (9)$$

where G^0 is the bulk Green function.

Results for the interlayer coupling, numerically calculated using a simple cubic one-band tight-binding model for the (100) orientation of the layers, are shown in Fig. 10 for two typical cases, each corresponding to one of the two situations described above³⁶. It is interesting to notice that as E_F moves above the edge of the well, the phase of the oscillations shifts by almost π , and its amplitude is very strongly reduced.

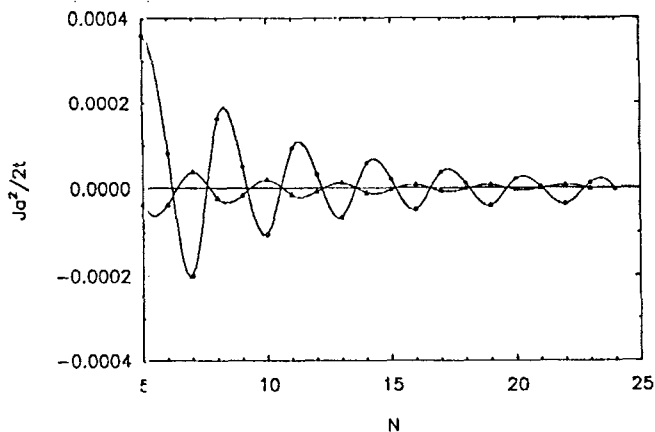


Figure 10.: Calculated values of the exchange coupling J for a simple cubic (100) one-orbital tight-binding model with nearest neighbour hopping constant t . J is plotted as a function of the number N of atomic layers in the spacer with the lattice constant a . The two curves correspond to different degrees of confinement $\epsilon = E_F/V$, where E_F is the Fermi level and V is the exchange splitting in the ferromagnetic layers. E_F is fixed at -2.5 (in units of $2t$); the circles correspond to strongly confined holes ($\epsilon = -1.0$) and triangles to weakly confined holes ($\epsilon = -6.25$).

The main conclusions for the one-band model are that the periods of the oscillation of the interlayer coupling are characteristic of the spacer metal, while the amplitude and phase of oscillations are very sensitive to the degree of confinement of the holes in the spacer, and hence depend on the matching between the spacer and the magnetic metals. Similar conclusions were obtained by Bruno⁴⁷ with a RKKY-like approach for a noble metal spacer, and experimentally, such a phase change was observed when Co and Fe are interchanged in Co/Cu, Fe/Cu multilayers²¹.

Oscillations of the interlayer exchange coupling show up in magnetoresistance measurements in which the observed change in resistance is between the sample at an applied low magnetic field and at a field which saturates its magnetization. When the sample is in a ferromagnetic configuration, it saturates at low field and no significant change in resistance is seen. Hence, distinguished peaks in the magnetoresistance measurements correspond to an antiferromagnetic configuration of the

multilayer.

VI. Giant magnetoresistance

The basic physical mechanism responsible for the giant magnetoresistance effect is the asymmetry in the scattering for electrons with different spins. In ferromagnetic transition metals such an asymmetry comes predominantly from the fact that the conduction electrons scatter into the d -band which has different density of final states for the two spins⁴⁸. The existence of available d -states at the Fermi energy acts as a trap for the conduction electrons; its effectiveness being proportional to the density of available d -states⁴⁹. In their original work⁴, Baibich et al. suggested that the magnetoresistance which they have observed was coming from spin-dependent scattering at the interfaces of the multilayers. Camley and Barnás⁵⁰ worked out a detailed semi classical theory based on the Boltzmann equation, first considering only interfacial scattering but later extending it to include also spin-dependent scattering in the bulk of the ferromagnetic layers⁵¹. Levy et al²⁵ used a quantum mechanical approach based on the Kubo formalism considering both spin-dependent interfacial and bulk scattering to calculate the magnetoresistance. Both Levy et al²⁵ and Barnás et al⁵¹ concluded that to explain the giant magnetoresistance effect a strong interfacial scattering is necessary. Edwards et al⁵², however, showed that this is not necessarily the case and obtained bulk scattering only⁵³. Whether bulk or interfacial scattering dominates probably depends on the system⁵⁴ and experimentally this question is still under investigation⁵⁵⁻⁵⁷. Here we shall describe the simplest theory⁵² with bulk scattering only, and when the current flows parallel to the layers.

We assume an sp conduction band common to all the layers running throughout the structure. Spin-flip scattering is neglected because the mean free path associated to it is usually very large in metals. In the absence of spin-flip scattering the two spin channels are independent and carry current in parallel. A free conduction electron with spin σ travelling through the structure experiences regions with different local resistivities, because, irrespectively of what precisely causes the scattering and even if we assume a uniform density of scattering centers throughout the structure, it is scattered at a rate which is largely determined by the local density of final states at the Fermi energy. We call ℓ_{\min} and ℓ_{\max} the mean free paths for minority and majority spin electrons in the ferromagnetic layers and ℓ_s the mean free path for both spins in the non-magnetic spacer metal. Consider for example a CoCu superlattice: in Cu the d bands are well below the Fermi energy and ℓ_{Cu} is large. In Co, however, although the majority d band is full (which is similar to Cu), the Fermi level lies near a peak in the minority spin density of states, hence $\ell_{\text{maj}}^{\text{Co}} \gg \ell_{\text{min}}^{\text{Co}}$. Therefore, the local resistivities (which are proportional to the inverse of the

local mean free paths) are different for electrons with different spins and depend on whether the multilayer is on a ferromagnetic or antiferromagnetic configuration. In Fig. 11 the distribution of local resistivities in the magnetic superlattice cell is shown schematically for each spin channel and for the ferromagnetic and antiferromagnetic configurations of the multilayer.

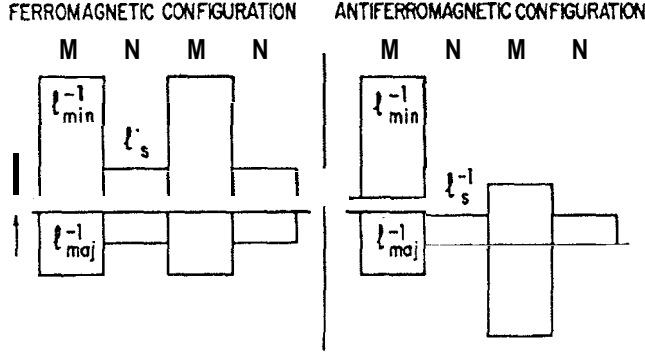


Figure 11.: Schematic representation of the distribution of local mean free paths ℓ^{-1} in the magnetic unit cell for the ferromagnetic and antiferromagnetic configurations of the magnetic layers. Both the resistivities in the spin \uparrow and spin \downarrow channels are shown. M and N denote, respectively, the magnetic and nonmagnetic layers.

When the current flows parallel to the layers it is instructive to consider two extreme limits: First, when the longest mean free path is much shorter than any of the layer thicknesses. In this case, electrons of a given spin will hardly sample different layers, which means that the layers will behave essentially as resistors in parallel. It is then clear that, in this case, there will be no magnetoresistance effect, i.e. $\Delta R/R \approx 0$, because the amount of high and low resistivities channels to be added in parallel will be exactly the same for both configurations of the multilayer. The second, and opposite limit, is when the mean free paths are much longer than the layer thicknesses. In this case, electrons of a given spin will sample many layers and will experience an average resistivity. One way of generally working out this average for superlattices is by numerically solving the Boltzmann equation with continuity and periodic boundary conditions imposed on the distribution function^{52,53}. However, in the very long mean free path limit, a conduction electron with spin σ shall equally sample all the layers and will experience a very simple average resistivity. More specifically, in such an extreme limit, the average resistivity for each spin in the antiferromagnetic configuration will be proportional to

$$(M\ell_{\min}^{-1} + M\ell_{\text{maj}}^{-1} + 2N\ell_s^{-1})/(2M + 2N), \quad (10)$$

whereas in the ferromagnetic configuration the corresponding average resistivities will be proportional to

$$(M\ell_{\text{maj}}^{-1} + N\ell_s^{-1})/(M + N), \quad (11)$$

for \uparrow spins, and

$$(M\ell_{\min}^{-1} + N\ell_s^{-1})/(M + N), \quad (12)$$

for \downarrow spins, where M and N are the thicknesses of the magnetic and non-magnetic layers respectively. It is clear from these equations (or Fig. 11) that the lowest average resistivity occur for the \uparrow spin electrons in the ferromagnetic configuration. This channel then acts as a shunt, making $R_{\uparrow\uparrow}$ smaller than $R_{\uparrow\downarrow}$. Also, from these straightforward averages, it follows that $\Delta R/R$ is given by

$$\Delta R/R = \frac{(\alpha - \beta)^2}{4(\alpha + N/M)(\beta + N/M)}, \quad (13)$$

where $\alpha = \ell_s/\ell_{\min}$ and $\beta = \ell_s/\ell_{\text{maj}}$. This very simple analytic formula, although valid only in the limit of very long mean free paths, helps to understand several of the magnetoresistance features observed in metallic multilayers. It is clear that for fixed α, β and $M\Delta R/R$ decreases as a function of N . Actually, we can see in Fig. 12 that Eq. 13 provides a good fit to the experimental data for reasonable values of the parameters α and β .

It is also clear that to obtain a large $\Delta R/R$ we need N/M as small as possible, ℓ_s as large as possible, and principally either α/β or β/α as large as possible. This explains why CoCu with both large ratio α/β and ℓ_s is such good a combination to produce large magnetoresistance effect. If Co is substituted by Fe, i.e. if a FeCu superlattice is considered, the situation is slightly different. The Fermi level in Fe lies in a dip of the minority spin density of states and $\ell_{\text{maj}}^{\text{Fe}} < \ell_{\min}^{\text{Fe}}$ hence $(\beta/\alpha)_{\text{Fe}} > 1$. However, the important thing is that the ratio $(\beta/\alpha)_{\text{Fe}}$ (roughly estimated from bulk density of states calculations⁵⁸) is smaller than the corresponding ratio $(\alpha/\beta)_{\text{Co}}$, causing the magnetoresistance of Fe/Cu to be smaller than that of Co/Cu as observed⁵⁹.

When impurities are added to the spacer metal turning it into an alloy, for a fixed M and N the ratio (α/β) associated to the bulk ferromagnetic metal is kept essentially constant but ℓ_s changes. In the low impurity concentration limit the decrease in ℓ_s is proportional both to the impurity concentration x and to the strength of the impurity scattering potential. Therefore, $\Delta R/R$ decreases with increasing x , and the decrease is more pronounced for impurities with larger $|\Delta z|$, where $|\Delta z|$ is the difference between the atomic numbers of the two alloy components. This was observed⁵⁹ in $\text{Fe}/(\text{X}_x\text{Cr}_{1-x})$ superlattices for $X = \text{Ti, V, Mn}$ (among others elements), and analyzed along these lines by Edwards et al⁶⁰. The situation when impurities are added to the ferromagnetic metal is more subtle. It is well known that impurities in ferromagnetic transition metals can produce significant changes to their electronic structure and these changes may be very different for the two spins directions. Virtual bound states may pass through the Fermi level,

split off from the bands; screening effectiveness is usually spin dependent and may vary, among other things according to the impurity type, and as to whether the matrix is a strong or a weak ferromagnet^{48,61-63}. As consequence, alloying the ferromagnet generally affect differently the density of states for electrons with different spins, and in many cases drastically changes both the magnetic and the transport properties of the ferromagnet. Feit and Campbell⁶⁴ have made an extensive and detailed investigation of the effect of diluted impurities in the transport properties of bulk ferromagnetic transition metals. They have shown that ℓ_{maj} and ℓ_{min} (hence the ratio α/β) may vary considerably according to the combination of the alloy components. The extent to which the changes in the magnetoresistance correlate to the changes in the alloy density of states as different alloy constituents are chosen for the ferromagnetic layers would be a good test to verify the importance of the present mechanism.

The simple formula on which we are basing our discussion obviously has limitations. It is valid when all the mean free paths are longer than the superlattice cell but this is not true in many cases. For example, Eq. 13 indicates that $\Delta R/R$ increases with increasing M (saturating at a value $(a-\beta)^2/4\alpha\beta$ when $M \rightarrow \infty$), but it clearly stops being valid when $h\lambda$ is longer than the shortest mean free path. In this case, as previously mentioned, we have to solve the Boltzmann equation to work out properly the average resistivities sampled by the conduction electrons with different spins. The shorter the mean free paths, relative to the layer thicknesses, the narrower will be the region effectively sampled, which causes the magnetoresistance to decrease. Therefore, the magnetoresistance may initially increase with increasing M but it should reach a maximum and then decrease as M gets longer and we deviate further from the uniform sampling and approach its opposite limit where the magnetoresistance is zero. A simple calculation shows that large deviations from the uniform sampling limit occur for mean free paths shorter than approximately $1/4^{\text{th}}$ of the superlattice cell⁵². In a Co/Cu superlattice for example, a more refined theoretical analysis⁵³ of the data based on the solution of the Boltzmann equation gives $\ell_{\text{min}} \simeq 12 \text{ \AA}$, $\ell_{\text{maj}} \simeq 130 \text{ \AA}$ and $\ell_s \simeq 260 \text{ \AA}$. The full solution shows that in $\text{Co}(M)\text{Cu}(9 \text{ \AA})$ superlattices $\Delta R/R$ passes through a maximum at $M \simeq \ell_{\text{min}}$, whereas the form of $\Delta R/R$ as a function of N does not depend much on ℓ_{min} for $M < \ell_{\text{min}}$. The maximum at $M \simeq 12 \text{ \AA}$ in Co_MCu_9 superlattices indicates that for $M > 12 \text{ \AA}$ significant deviations from the uniform sampling becomes important, which is consistent with ℓ_{min} being less than $1/4^{\text{th}}$ of the magnetic superlattice cell. It is therefore clear that for a larger Cu spacer as in $\text{Co}_M\text{Cu}_{20}$ superlattices the maximum, if it occurs, would certainly be at a value of $M < 12 \text{ \AA}$ (possibly at $M < 4 \text{ \AA}$) as the experimental data of Mosca⁶⁵ suggests.

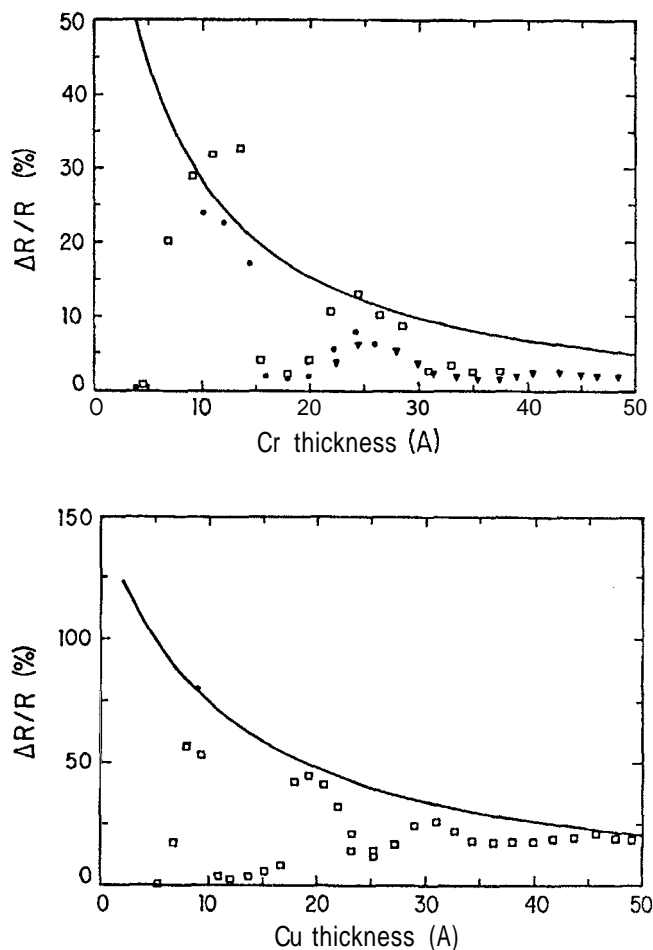


Figure 12.: (a) Dependence of $\Delta R/R$ on Cr thickness for $\text{Fe}(20 \text{ \AA})/\text{Cr}(t_{\text{Cr}})$ superlattices. The full line is calculated by Eq. 13 with $a = .4$ and $\beta = 2$, and the experimental data is taken from ref. [G]. (b) Dependence of $\Delta R/R$ on Cu thickness for $\text{Co}(10 \text{ \AA})/\text{Cu}(t_{\text{Cu}})$ superlattices. The full line is calculated by Eq. 13 with $a = 10$ and $\beta = 1.3$, and the experimental data is taken from Parkin et al²³.

Let us now briefly discuss the role played by interfacial scattering in the magnetoresistance effect. Generally there will be a mismatch on the bottoms of the conduction bands of the two metals separated by an interface. In this situation, the conduction electrons would experience a potential step when crossing the interfaces. However, for interfaces between two transition metals or between transition and a noble metals these steps are small compared to the Fermi energy hence, as a reasonable approximation, they may be neglected. Nevertheless, when the interface is not sharp the two metals mix and in the most simple picture will form an alloy. As we previously mentioned, alloying a ferromagnet may significantly alter ℓ_{min} and ℓ_{maj} hence the asymmetry ratio α/β . Other effects due to lattice spacing mismatch between the two metals, existence of terraces, structural defects etc... may also contribute

to make the asymmetry in scattering at the interfaces be very different from its corresponding bulk value. A transport theory including a detailed description of the possible inhomogeneities at the interfaces would certainly be too laborious. A very simple approach is to treat the interface as a third material in which the associated mean free paths ℓ_{\min} and ℓ_{\max} are considered as arbitrary parameters. Such treatment ignores variations in the composition within the interface width, which is reasonable when both mean free paths are long on the scale where such variations occur. In this case, the Boltzmann equation needs to be solved for a eight-component system instead of four when interface scattering is neglected. Within this straightforward generalization, the two additional parameters ℓ_{\min}^i and ℓ_{\max}^i associated with the interfaces may also be determined so as to fit experimental data, and, in this way, the relative importance between bulk and interface scattering could be estimated for a particular system. We should bear in mind that the magnetoresistance effect depends on the width of the region effectively sampled by the conduction electrons. To obtain the effect it is essential that at least two magnetic layers are sampled (from Fig. 11 we can clearly see that if pairs of magnetic/non-magnetic layers are treated as resistors in parallel there will be no magnetoresistance effect). Therefore, the relative importance between bulk and interfacial scattering $\Delta R/R$ may also depend on the relation between the mean free paths and the layer thicknesses, because in some cases it may happen that only a fraction of the magnetic layers are effectively sampled. Clearly, better experimental characterization and control of interface quality will be decisive on establishing whether bulk or interface scattering dominates in each case. Reliable theoretical calculations of the electronic structures are also very important to understand the changes which occur at the interfaces and how they correlate to the asymmetry in the scattering of electrons with different spins.

Acknowledgments

Most of the theoretical ideas and calculations presented here by one of us (RBM) are the product of an enjoyable collaboration with D. M. Edwards and J. Mathon. He would like to thank them for their constant teachings and for making his learning of this subject so pleasurable. Very useful discussions with Dr. J. d'Albuquerque e Castro, Dr. Murielle Villaret Prof. A. A. Gomes and Prof. A. Fert are also gratefully acknowledged by the authors. We acknowledge partial financial support provided by CNPq and FINEP.

References

1. P. J. Flanders, *J. Appl. Phys.* 63, 3940 (1988).
2. L. M. Falicov, D. T. Pierce, S. D. Bader, R. Gronsky, K. B. Hathaway, H. J. Hopster, D. N. Lambeth, S. S. P. Parkin, G. Prinz, M. Saloion, I. K. Schuller, and R. H. Victora, *J. Mater. Res.* 5, 1299 (1990).
3. R. Krishnan, H. Lassri, R. Porte, R. Tessier, and P. Renaudin, *Appl. Phys. Lett.* 59, 3649 (1991); R. Krishnan, M. Porte, and R. Tessier, *IEEE Trans. Magn.* 26, 2727 (1989).
4. M. N. Baibich, J. R. Broto, A. Fert, F. Nguyen Van Dau, F. Petroff, P. Etienne, G. Creuzet, A. Friederich and J. Chazelas, *Phys. Rev. Lett.* 61, 2472 (1988).
5. P. Grünberg, R. Schreiber, Y. Pang, R. N. Brodsky and H. Sowers, *Phys. Rev. Lett.* 571, 2412 (1986).
6. S. S. P. Parkin, N. More and K. P. Roche, *Phys. Rev. Lett.* 641, 2304 (1990).
7. J. F. M. Borgcs, G. Tosin, L. F. Schelp, N. Matoso, S. R. Teixeira, D. H. Mosca, \I. H. Schreiner (to be published).
8. H. J. G. Draaisma, Thesis (Eindhoven 1988) unpublished.
9. F. J. A. den Broeder, H. J. G. Draaisma, H. C. Donkersloot, and W. J. R. de Jonge, *J. Appl. Phys.* 61, 4317 (1987).
10. U. Gradman and S. F. Alvarado, *Surface Crystallography*, (Springer Verlag, Berlin, 1979).
11. A. Barthélemy, A. Fert, R. N. Baibich, S. Hadjoudj, F. Petroff, P. Etienne, R. Cabanel, S. Lequien, F. Nguyen Van Dau, and G. Creuzet, *J. Appl. Phys.* 67, 5908 (1990).
12. C. Liu, E. R. Moog, and S. R. Bader, *Phys. Rev. Lett.* 60, 2422 (1988); T. Katayama, Y. Suzuki, H. Awano, Y. Nishirara, and N. Koshizuka, *Phys. Rev. Lett.* 60, 1426 (1988).
13. F. Nguyen Van Dau, A. Fert, P. Etienne, R. N. Baibich, J. M. Broto, G. Creuzet, A. Friederich, S. Hadjoudj, H. Hurdequint, and J. Massies, *J. Phys. (Paris) Colloq.* 49 C8, 1633 (1988).
14. P. Grünberg, S. Demokritov, A. Fuss, M. Vohl, and J. A. Wolf, *J. Appl. Phys.* 69, 4780 (1991).
15. S. T. Purcell, W. Folkerts, R. T. Jolinson, N. W. E. McGee, K. Jager, J. van de Stegge, W. B. Zeper, and W. Hoiving, *Phys. Rev. Lett.* 67, 903 (1991).
16. S. Demokritov, J. A. Wolf, and P. Grünberg, *Europhys. Lett.* 15, 881 (1991); P. Grünberg, *J. Magn. Mater.* 104-107, 1734 (1992).
17. J. Unguris, R. J. Cellota, and D. T. Pierce, *Phys. Rev. Lett.* 67, 140 (1991).
18. A. T. Johnson, S. T. Purcell, N. W. E. McGee, R. Coehoorn, J. van de Stegge, and W. Hoiving, *Phys. Rev. Lett.* 68, 2688 (1992); and references therein.
19. W. F. Egelhoff Jr., and M. T. Kief, *Phys. Rev. B* 45, 7795 (1992); see also ref. 56.

20. F. Petroff, A. Barthélemy, D. H. Mosca, D. K. Lottis, A. Fert, P. A. Schroeder, W. P. Pratt Jr., R. Lalce, and S. Lequien, *Phys. Rev. B* **44**, 5355 (1991).
21. K. Fujis, *Proc. Camb. Phil. Soc.* **34**, 2000 (1938); E. H. Sondheimer, *Adv. Phys.* **1**, 1 (1952).
22. P. F. Garcia and A. Suna, *J. Appl. Phys.* **54**, 2000 (1983).
23. D. H. Mosca, F. Petroff, A. Fert, P. A. Schroeder, W. P. Pratt Jr. and R. Laloe, *J. Magn. Magn. Mat.* **94**, L1 (1991); S. S. P. Parkin, R. Bhadra and K. P. Roche, *Phys. Rev. Lett.* **66**, 2152 (1991); A. Fert, A. Barthélemy, P. Etienne, S. Lequien, R. Laloe, D. K. Lottis, D. H. Mosca, F. Petroff, W. P. Pratt, and P. A. Schroeder, *J. Magn. Magn. Mater.* **104-107**, 1712 (1992).
24. W. P. Pratt Jr., S. F. Lee, J. R. Slaughter, R. Laloe, P. A. Schroeder, and J. Bass, *Phys. Rev. Lett.* **66**, 3060 (1991).
25. P. R. Levy, S. Zhang, and A. Fert, *Phys. Rev. Lett.* **65**, 1643 (1990).
26. T. Folkerts, W. Hoing, and W. Coene, *J. Appl. Phys.* **71**, 362 (1991).
27. S. Zhang, and P. M. Levy (preprint).
28. C. Carbone and S. F. Alvarado, *Phys. Rev. B* **36**, 2433 (1987).
29. B. Heinrich, Z. Celinski, J. F. Cochran, W. B. Muir, J. Rudd, Q. M. Zhong, A. S. Arrot, K. Myrtle and J. Kisliner, *Phys. Rev. Lett.* **64**, 673 (1990); W. R. Bennet, W. Schwarzacher and W. F. Egelhoff Jr., *Phys. Rev. Lett.* **65**, 3169 (1990).
30. H. Hasegawa, *Phys. Rev. B* **42**, 2368 (1990); **43**, 10803 (1991).
31. P. R. Levy, K. Ounadjela, S. Ziang, Y. Wang, C. B. Sommers and A. Fert, *J. Appl. Phys.* **67**, 5914 (1990).
32. F. Herman, J. Sticlit and M. Van Schilfgaarde, *J. Appl. Phys.* **69**, 4783 (1991). *Magnetic Thin Films Multilayers and Surfaces*, ed by S. S. P. Parkin et al, AIRS Symposium Proceedings 1992, Vol. 231 (to be published).
33. D. Stoeffler and F. Gautier, *Progr. Theor. Phys. Suppl.* **101**, 139 (1990); *J. of Magn. and Magn. Mater.* **104-107**, 1819 (1992).
34. D. M. Edwards, J. Mathon, R. B. Muniz and M. S. Phan, *J. Phys.: Condens. Matter* **3**, 3941 (1991).
35. D. M. Edwards, J. Mathon, R. B. Muniz and M. S. Phan, *Phys. Rev. Lett.* **67**, 493 (1991); **67**, 1476(E) (1991).
36. D. M. Edwards, J. Mathon and R. B. Munia, *Physica Scripta* 1992 (to be published); J. Mathon, Murielle Villeret, D. M. Edwards, and R. B. Muniz, *J. of Magn. and Magn. Mater.* (to be published); J. Mathon, Murielle Villeret, and D. M. Edwards, *J. Phys.: Condens. Matter* (to be published).
37. S. J. Frisken and D. J. Miller, *Phys. Rev. Lett.* **57**, 2971 (1986).
38. W. Baltensberger and J. S. Helman, *Appl. Phys. Lett.* **57**, 2954 (1990).
39. Y. Wang, P. M. Levy and J. L. Fry, *Phys. Rev. Lett.* **65**, 2732 (1990).
40. P. Bruno and C. Chiappert, *Phys. Rev. Lett.* **67**, 1602 (1991).
41. C. Lacroix and J. P. Gavigan, *J. Magn. Magn. Mater.* **93**, 413 (1991).
42. L. M. Roth, H. J. Zeiger and T. A. Kaplan, *Phys. Rev.* **149**, 519 (1966); F. Herman and R. Schirreff (preprint).
43. R. Coehoorn, *Phys. Rev. B* **44**, 9331 (1991).
44. C. Chappert and J. P. Renard, *Europhys. Lett.* **15**, 553 (1991).
45. Y. Yafet, *J. Appl. Phys.* **61**, 4058 (1987).
46. C. E. T. Gonçalves da Silva and L. M. Falicov, *J. Phys. C: Sol. Stat. Phys.* **5**, 63 (1972).
47. P. Bruno (preprint).
48. N. F. Mott, *Adv. Phys.* **13**, 325 (1964).
49. J. M. Ziman, *Electrons and Phonons - The International Series of Monographs on Physics*, ed. by N. F. Mott, E. C. Bullard and D. Wilkinson (Oxford University Press, Oxford, 1960).
50. R. E. Camley and J. Barnás, *Phys. Rev. Lett.* **63**, 664 (1989).
51. J. Barnás, A. Fuss, R. E. Camley, P. Grunberg and W. Zinn, *Phys. Rev. B* **42**, 8110 (1990).
52. D. M. Edwards, R. B. Muniz and J. Mathon, *IEEE Transactions on Magnetics* **27**, 3548 (1991).
53. D. M. Edwards, J. Mathon, R. B. Muniz and S. S. P. Parkin, *J. Magn. Magn. Mat.*, 1992 (to be published).
54. B. Dieny, V. S. Speriosu, S. Metin, S. S. P. Parkin, B. A. Gurney, P. Baumgart and D. R. Wilhoit, *J. Appl. Phys.* **69**, 4774 (1991).
55. E. E. Fullerton, D. M. Kelly, J. Guimpel, I. K. Schuller and Y. Bruynseraede, *Phys. Rev. Lett.* **68**, 859 (1992).
56. D. Greig, M. J. Hall, C. Hammond, B. J. Hickey, H. P. Ho, M. A. Howson, M. J. Walker, N. Wiser and D. G. Wright, *J. Magn. Magn. Mat.* 1992 (to be published).
57. S. S. P. Parkin *Appl. Phys. Lett.* **61**, 1358 (1992).
58. V. L. Moruzzi, J. F. Janak and A. R. Williams, *Calculated Electronic Properties of Metals* (Pergamon, New York, 1978).
59. K. Takanashi, Y. Obi, N. Tsuda and H. Fujimori (preprint).
60. D. M. Edwards, J. Mathon, and R. B. Muniz (to be published).
61. J. Friedel, *Nuovo Cim. Suppl.* **8**, 287 (1958).
62. W. Marshall, *J. Phys. C* **1**, 88 (1968).
63. D. M. Edwards, *Electrons in Disordered Metals and Metallic Surfaces*, Ed. P. Phariseau et al., NATO ASI Series B: Physics, vol. 42, (Plenum, New York, 1979) Vol. 42.

64. A. Fert and I. Campbell, *J. Phys. F: Metal Physics* **6**, 849 (1976); I. Campbell and A. Fert, *Ferromagnetic Materials*, ed. E. P. Wohlfarth, (North Holland, Amsterdam, 1984) Vol. **3**.
65. D. Il. Mosca, PhD Thesis, Universidade Federal do Rio Grande do Sul, Brazil (1992).